JOURNAL OF THEORETICAL AND APPLIED MECHANICS
48, 2, pp. 397-413, Warsaw 2010

THE INFLUENCE OF WING TRANSVERSE VIBRATIONS ON DYNAMIC PARAMETERS OF AN AIRCRAFT

Michał Wachłaczenko

Air Force Institute of Technology, Aero-Engines Division, Warsaw, Poland

e-mail: michal.wachlaczenko@itwl.pl

The paper presents numerical analysis of airplane parameters of motion during wing transverse vibrations of an average commercial airplane. The mathematical model of the airplane motion including a system of twelve ordinary differential equations was employed. Using available publications and M28 "Bryza" airplane geometrical and mass relationships, a computer code evaluating parameters of the motion was developed. In order to take the wing transverse vibrations under consideration, the way of wing displacements in the aircraft-fixed system of coordinates was elaborated as well as vibration amplitude and frequency were assumed. The analysis covered two cases of wing transverse vibrations: bending of both wing halves in phase and in counter-phase. On the basis of the obtained results, some conclusions referring the airplane dynamic properties during wing vibrations were formulated.

Key words: wing vibrations, aircraft, sumulation

1. Introduction

There are several forces and moments acting on the structure of an airplane during its flight in disturbed earth's atmosphere. Because of the nature of the interactions, they can be divided into two groups. The first group of airframe loadings is connected with the influence of the medium surrounding and affecting the external surfaces of the airplane. The second one, speaking generally, are the internal interactions of the airframe and elasticity forces. They both create aeroelastic phenomena.

Analysis of stability and steerability properties employs simplification that the airplane is a 6DOF (degree of freedom) rigid body. An assumption is made that all the airframe elements occupy an invariant position toward one another through the whole time of analysis. This is one sufficient condition to determine

the mass and aerodynamic forces as well as moments acting on the aircraft during steady flight in the atmosphere.

The phenomenon of aeroelasticity has accompanied the process of creation of airframes since the beginning of aviation. Varying loadings due to flow disturbances change the aerodynamic loads. This leads to vibrations of lifting surfaces (wings, tailplane) as well as bigger assemblies like the aircraft tail with the tailplane. Furthermore, the forces produced by wing vibrations are transferred through joints to the fuselage inducing its bending or/and twisting.

Aircraft vibrations cause premature wear and tear of elements and assemblies. A proper material and structure selection allow the airframe to work below the elastic limits. Exceeding the permissible loads during flight may lead to permanent airframe deformation. Loads surpassing the maximum permissible loading cause airframe failure and crash.

Vibrations of the lifting surfaces have significant influence on the airplane dynamic parameters. For example, in the commercial aviation varying aerodynamic forces and moments acting on the airplane, as an effect of structure vibrations, produce variable gravity loads lowering the journey comfort. Those factors worsen concentration of the air-crew and bring fatigue to passengers.

The phenomena mentioned above are a kind of impulse for many research centers worldwide to make particular investigations aimed at minimising the adverse operational conditions and increasing the flight safety. Carrying out laboratory experimental research is usually insufficient, but in-flight investigations can be sometimes very dangerous. Therefore, parallel creation of the airframe vibration mathematical models is highly reasonable. This way, one can lower the costs of the research and the hazard of disaster.

2. Equations of motion of the airplane

Spatial motion of the airplane treated as a rigid body is described by twelve nonlinear ordinary differential equations. Solving them in a general form is a complex problem which has not been accomplished so far. In practice, engineering calculations employ approximate methods on the basis of computer technology.

There are many external forces and moments of forces acting on the aircraft during flight, which are complex functions of motion parameters as well as geometrical and mass quantities of the investigated object. Additional forces and moments of forces are generated by displacements of control surfaces.

The assumed simplification are:

- the airplane is a rigid body with constant mass, constant moment of inertia and invariable position of the centre of mass;
- control surfaces are stiff and their axes of rotation have invariable position against the airplane;
- the plane Oxz is the geometrical, inertial and aerodynamic symmetry plane.

The gyrostatic moment produced by elements of revolving turbo-prop engines is taken into consideration in the equations of motion.

Figure 1 presents the systems of coordinates used in numerical analysis.

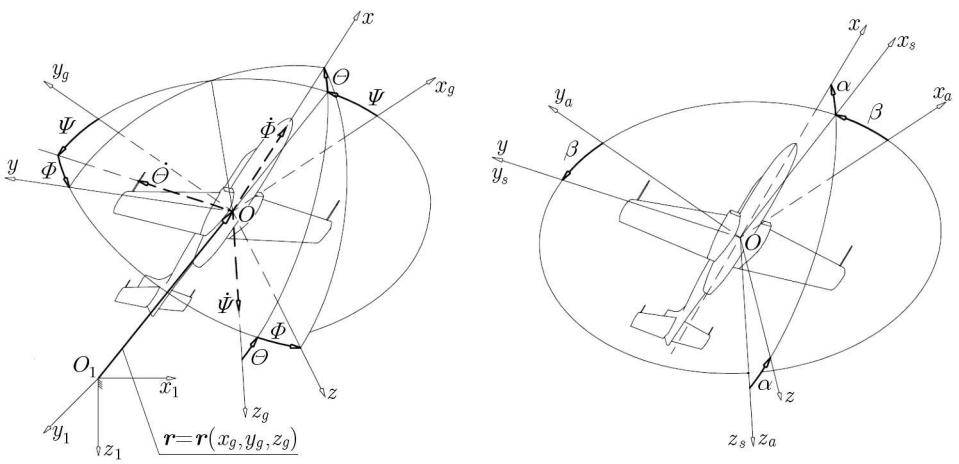

Fig. 1. Systems of coordinates and angles defining their mutual position

Mutual orientation of the coordinate systems are defined by the following angles: angle of attack α; angle of slideslip β; aircraft roll angle Φ; aircraft pitch angle Θ; aircraft yaw angle Ψ.

Performing rotations successively by Euler angles Ψ, Θ and Φ from $Ox_gy_gz_g$ to $Oxyz$, the transformation matrix is determined

$$\begin{bmatrix} x \\ y \\ z \end{bmatrix} = \mathbf{L}_{s/g} \begin{bmatrix} x_g \\ y_g \\ z_g \end{bmatrix} \tag{2.1}$$

where

$$\mathbf{L}_{s/g} = \tag{2.2}$$
$$= \begin{bmatrix} \cos\Psi\cos\Theta & \sin\Psi\cos\Theta & -\sin\Theta \\ \cos\Psi\sin\Theta\sin\Phi - \sin\Psi\cos\Phi & \sin\Psi\sin\Theta\sin\Phi + \cos\Psi\cos\Phi & \cos\Theta\sin\Phi \\ \cos\Psi\sin\Theta cos\Phi + \sin\Psi sin\Phi & \sin\Psi\sin\Theta\cos\Phi - \cos\Psi\sin\Phi & \cos\Theta\cos\Phi \end{bmatrix}$$

Performing rotations by $-\beta$ and α angles from $Ox_ay_az_a$ to $Oxyz$, another transformation matrix is determined

$$\begin{bmatrix} x \\ y \\ z \end{bmatrix} = \mathbf{L}_{s/a} \begin{bmatrix} x_a \\ y_a \\ z_a \end{bmatrix} \tag{2.3}$$

where

$$\mathbf{L}_{s/a} = \begin{bmatrix} \cos\alpha\cos\beta & -\cos\alpha\sin\beta & -\sin\alpha \\ \sin\beta & \cos\beta & 0 \\ \sin\alpha\cos\beta & -\sin\alpha\sin\beta & \cos\alpha \end{bmatrix} \tag{2.4}$$

2.1. Equations of the airplane translational motion

The equation of motion for the center of mass is

$$m\frac{d\boldsymbol{V}}{dt} = \boldsymbol{F} \tag{2.5}$$

and can be written in a scalar form in the airplane-fixed system of coordinates $Oxyz$

$$m(\dot{u} + qw - rv) = X \qquad m(\dot{v} + ru - pw) = Y \qquad m(\dot{w} + pv - qu) = Z \tag{2.6}$$

where: m is the airplane mass; $\boldsymbol{V} = [u, v, w]^\top$ – vector of absolute velocity of the centre of mass of the airplane; $\boldsymbol{\Omega} = [p, q, r]^\top$ – vector of rotational velocity in the mobile system of coordinates; $\boldsymbol{F} = [X, Y, Z]^\top$ – vector of external forces acting on the airplane.

Equations (2.6) are to be evaluated in the flow coordinate system $Ox_ay_az_a$ for the sake of simplicity of determination of aerodynamic forces in this system. Therefore, the velocity vector has only one component $u_a = V$ and equations (2.6) gain the following form

$$m\dot{V} = X_a \qquad mr_aV = Y_a \qquad -mq_aV = Z_a \tag{2.7}$$

Assuming that the rotational velocity of the airplane-fixed system $Oxyz$ in the inertial system is equal to $\boldsymbol{\Omega}_s$ and the velocity of the fixed coordinate

system $Oxyz$ in the flow coordinate system $Ox_ay_az_a$ is known, allows one to determine the rotational velocity of the $Ox_ay_az_a$ system in the inertial system (Issac, 1995)

$$\boldsymbol{\Omega}_a = \boldsymbol{\Omega}_s + \boldsymbol{\Omega}_{s/a} = \boldsymbol{\Omega}_s + \dot{\boldsymbol{\alpha}} + \dot{\boldsymbol{\beta}} \tag{2.8}$$

Considering that:

– $\boldsymbol{\Omega}_s$ vector in the $Oxyz$ system is $\boldsymbol{\Omega}_s = [p, q, r]^\top$;

– $\dot{\boldsymbol{\beta}}$ vector in the $Ox_ay_az_a$ system is $\dot{\boldsymbol{\beta}} = [0, 0, \dot{\boldsymbol{\beta}}]^\top$;

– $\dot{\boldsymbol{\alpha}}$ vector in the $Oxyz$ system is $\dot{\boldsymbol{\alpha}} = [0, -\dot{\boldsymbol{\alpha}}, 0]^\top$;

and making use of transformations matrix (2.4), on the basis of (2.8), we get

$$\begin{aligned} p_a &= p\cos\alpha\cos\beta + (q - \dot{\boldsymbol{\alpha}})\sin\beta + r\sin\alpha\cos\beta \\ q_a &= -p\cos\alpha\sin\beta + (q - \dot{\boldsymbol{\alpha}})\cos\beta - r\sin\alpha\sin\beta \\ r_a &= -p\sin\alpha + r\cos\alpha + \dot{\boldsymbol{\beta}} \end{aligned} \tag{2.9}$$

The third equation of (2.7) considers the aerodynamic force P_{za} as a part of the force Z_a depending, among others, on the rate of change of the airplane angle of attack. Thus it is calculated as follows

$$Z_a = Z_{a\,st} + Z_a^{\dot{\alpha}}\dot{\alpha} \tag{2.10}$$

Inserting systems (2.9) and (2.10) into equations of motion (2.7) and transformaing, one obtains

$$\begin{aligned} \dot{V} &= \frac{1}{m}(X_s\cos\beta + Y_s\sin\beta) \\ \dot{\alpha} &= \frac{1}{\cos\beta - \frac{Z_S^{\dot{\alpha}}}{mV}}\Big[\frac{Z_{S\,st}}{mV} + q\cos\beta - (p\cos\alpha + r\sin\alpha)\sin\beta\Big] \\ \dot{\beta} &= \frac{1}{mV}(Y_s\cos\beta - X_s\sin\beta) + p\sin\alpha - r\cos\alpha \end{aligned} \tag{2.11}$$

2.2. Equations of rotary motion of the airplane

The differential vector equation for change of the total angular momentum is

$$\frac{d\boldsymbol{K}}{dt} = \boldsymbol{M} + \boldsymbol{M}_{gir} \tag{2.12}$$

where: $\boldsymbol{K} = \sum_i(\boldsymbol{r}_i \times m_i\boldsymbol{V}_i)$ is the total angular momentum with respect to the given reference point; $\boldsymbol{M} = [L, M, N]^\top$ – vector of moment of forces acting on the airplane; $\boldsymbol{M}_{gir} = J\boldsymbol{\omega} \times \boldsymbol{\Omega}$ – gyrostatic moment; J – moment of inertia of the engine rotor; $\boldsymbol{\omega} = [\omega, 0, 0]^\top$ – angular velocity of the engine rotor.

Components of the gyrostatic moment, according to Kowaleczko (2003), are defined as

$$\boldsymbol{M}_{gir} = [L_{gir}, M_{gir}, N_{gir}]^{\top} = [0, -J\omega r, J\omega q]^{\top} \tag{2.13}$$

As the Oxz surface is the airplane geometrical, inertial and aerodynamic symmetry plane and the engine rotors revolve with the angular velocity ω along an axis parallel to the Ox axis, the scalar form of equation (2.12) in the airplane-fixed system of coordinates $Oxyz$ is

$$\begin{aligned} &I_x\dot{p} - (I_y - I_z)qr - I_{xz}(\dot{r} + pq) = L \\ &I_y\dot{q} - (I_z - I_x)pr - I_{xz}(r^2 - p^2) = M - J\omega r \\ &I_z\dot{r} - (I_x - I_y)pq - I_{xz}(\dot{p} - qr) = N + J\omega q \end{aligned} \tag{2.14}$$

Transforming system (2.14)

$$\begin{aligned} \dot{p} &= \frac{1}{I_X I_Z - I_{XZ}^2}\{[L + (I_Y - I_Z)qr + I_{XZ}pq]I_Z + \\ &\quad +[N + J\omega q + (I_X - I_Y)pq - I_{XZ}qr]I_{XZ}\} \\ \dot{q} &= \frac{1}{I_Y}[M - J\omega r + (I_Z - I_X)rp + I_{XZ}(r^2 - p^2)] \\ \dot{r} &= \frac{1}{I_X I_Z - I_{XZ}^2}\{[L + (I_Y - I_Z)qr + I_{XZ}pq]I_{XZ} + \\ &\quad +[N + J\omega q + (I_X - I_Y)pq - I_{XZ}qr]I_X\} \end{aligned} \tag{2.15}$$

2.3. Modified equations of motion used in numerical analysis

To equations (2.11) and (2.15) we need to add equations allowing for definition of the current Euler angles (kinematic relations) of the airplane

$$\begin{aligned} &\dot{\Phi} = p + (r\cos\Phi + q\sin\Phi)\tan\Theta \qquad \dot{\Theta} = q\cos\Phi - r\sin\Phi \\ &\dot{\Psi} = (r\cos\Phi + q\sin\Phi)\frac{1}{\cos\Theta} \end{aligned} \tag{2.16}$$

and equations determining the position of the airplane centre of mass in the gravitational system of coordinates $Ox_gy_gz_g$

$$\begin{aligned} \dot{x}_g &= V[\cos\alpha\cos\beta\cos\Theta\cos\Psi + \sin\beta(\sin\Phi\sin\Theta\cos\Psi - \cos\Phi\sin\Psi) + \\ &\quad + \sin\alpha\cos\beta(\cos\Phi\sin\Theta\cos\Psi + \sin\Phi\sin\Psi)] \\ \dot{y}_g &= V[\cos\alpha\cos\beta\cos\Theta\sin\Psi + \sin\beta(\sin\Phi\sin\Theta\sin\Psi + \cos\Phi\cos\Psi) + \\ &\quad + \sin\alpha\cos\beta(\cos\Phi\sin\Theta\sin\Psi - sin\Phi\cos\Psi)] \\ \dot{z}_g &= V[-\cos\alpha\cos\beta\sin\Theta + \sin\beta\sin\Phi\cos\Theta + \sin\alpha\cos\beta\cos\Phi\cos\Theta] \end{aligned} \tag{2.17}$$

Equations (2.11) and (2.15)-(2.17) create a set of twelve nonlinear ordinary differential equations describing spatial motion of the airplane treated as a rigid body with constant mass. The vector of motion parameters has the following components: V, α, β, p, q, r, Φ, Θ, Ψ, x_g, y_g, z_g.

3. Forces and moments acting on the airplane

The resultant vector of external forces which affect the airplane during flight (right-hand side of equation (2.5)) is a sum of the following forces

$$\boldsymbol{F} = \boldsymbol{Q} + \boldsymbol{T} + \boldsymbol{R} \tag{3.1}$$

where: $\boldsymbol{T}$ is the thrust force; $\boldsymbol{R}$ – aerodynamic force; $\boldsymbol{Q}$ – terrestrial gravity force.

The corresponding components of resultant external force (3.1) can be written as

$$X_a = Q_{x_a} + T_{x_a} + R_{x_a} \qquad Y_a = Q_{y_a} + T_{y_a} + R_{y_a} \qquad Z_a = Q_{z_a} + T_{z_a} + R_{z_a} \tag{3.2}$$

3.1. Gravity force $\boldsymbol{Q}$

The terrestrial gravity force Q acting on the airplane in the $Ox_g y_g z_g$ system has only one component $\boldsymbol{Q} = [0, 0, mg]^\top$. Using relations (2.2) and (2.4), these components in the $Ox_a y_a z_a$ system can be determined

$$\begin{bmatrix} Q_{x_a} \\ Q_{y_a} \\ Q_{z_a} \end{bmatrix} = \mathbf{L}_{s/a}^{-1} \mathbf{L}_{s/g} \begin{bmatrix} 0 \\ 0 \\ mg \end{bmatrix} = \\ = \begin{bmatrix} mg(-\cos\alpha\cos\beta\sin\Theta + \sin\beta\sin\Phi\cos\Theta + \sin\alpha\cos\beta\cos\Phi\cos\Theta) \\ mg(\cos\alpha\sin\beta\sin\Theta + \cos\beta\sin\Phi\cos\Theta - \sin\alpha\sin\beta\cos\Phi\cos\Theta) \\ mg(\sin\alpha\sin\Theta + \cos\alpha\cos\Phi\cos\Theta) \end{bmatrix} \tag{3.3}$$

3.2. Engine thrust force $\boldsymbol{T}$

Both engine propeller thrust vectors $\boldsymbol{T}_L$ and $\boldsymbol{T}_R$ lie in planes parallel and equidistant to the aircraft symmetry plane Oxz as well as parallel to the Ox

axis. In the $Oxyz$ system, $\boldsymbol{T}$ has only one component $\boldsymbol{T} = [T_L + T_P, 0, 0]^\top$. Using transformation matrix (2.4), the thrust force vector is obtained

$$\begin{bmatrix} T_{x_a} \\ T_{y_a} \\ T_{z_a} \end{bmatrix} = \mathbf{L}_{s/a}^{-1} \begin{bmatrix} T_L + T_P \\ 0 \\ 0 \end{bmatrix} = \begin{bmatrix} (T_L + T_P)\cos\alpha\cos\beta \\ -(T_L + T_P)\cos\alpha\sin\beta \\ -(T_L + T_P)\sin\alpha \end{bmatrix} \tag{3.4}$$

3.3. Aerodynamic force $\boldsymbol{R}$

Projections of the resultant aerodynamic R force on axes of the $Ox_ay_az_a$ system are

$$\begin{aligned} R_{x_a} &= -P_{xa} = -C_{xa}\frac{\rho V^2}{2}S \qquad R_{y_a} = -P_{ya} = -C_{ya}\frac{\rho V^2}{2}S \\ R_{z_a} &= -P_{za} = -C_{za}\frac{\rho V^2}{2}S \end{aligned} \tag{3.5}$$

where: C_{xa}, C_{ya}, C_{za} denote the drag, side, lift coefficients, respectively; ρ is the air density; S – wing (lifting surface) area.

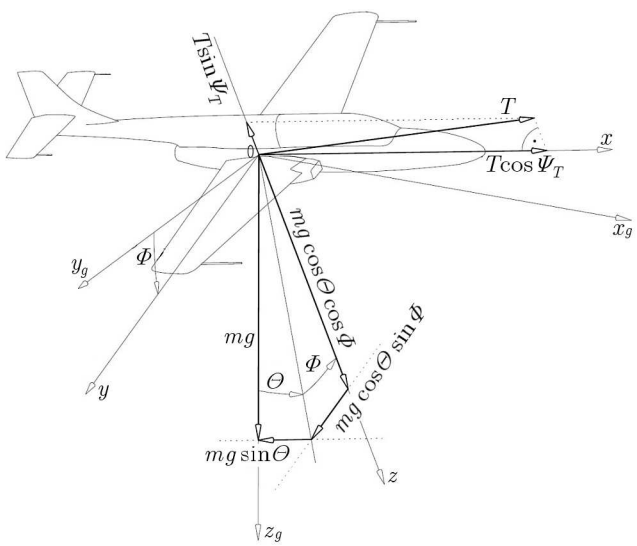

Fig. 2. Forces acting on the airplane

The moment $\boldsymbol{M} = [L, M, N]^\top$ on the right-hand side of equation (2.12) is the resultant moment affecting the airplane, whose components are defined as

$$L = C_l\frac{\rho V^2}{2}Sl \qquad M = C_m\frac{\rho V^2}{2}Sb_A \qquad N = C_n\frac{\rho V^2}{2}Sl \tag{3.6}$$

where: C_l, C_m, C_n are the roll, pitch, yaw moment coefficients, respectively; l – wing span; b_A – mean wing chord.

3.4. Coefficients of the aerodynamic force and moment

In this paper, experimentally obtained static aerodynamic characteristics $C_{xa}(\alpha, \mathrm{Ma})$, $C_{za}(\alpha, \mathrm{Ma})$, $C_m(\alpha, \mathrm{Ma})$ are used. Along with the determined derivatives they allow one to define final expressions defining force and moment coefficients:

- drag force: $C_{xa} = C_{xa}(\alpha, \mathrm{Ma})$
- side force: $C_{ya} = C_{ya}^{\beta}\beta + C_{ya}^{p}p + C_{ya}^{r}r + C_{ya}^{\delta_V}\delta_V + C_{ya}^{\delta_l}\delta_l$
- lift force: $C_{za} = C_{za}(\alpha, \mathrm{Ma}) + C_{za}^{\dot{\alpha}}\dot{\alpha} + C_{za}^{q}q + C_{za}^{\delta_H}\delta_H$
- rolling moment: $C_l = C_l^{\beta}\beta + C_l^{p}p + C_l^{r}r + C_l^{\delta_V}\delta_V + C_l^{\delta_l}\delta_l$
- pitching moment: $C_m = C_m(\alpha, \mathrm{Ma}) + C_m^{\dot{\alpha}}\dot{\alpha} + C_m^{q}q + C_m^{\delta_H}\delta_H$
- yawing moment: $C_n = C_n^{\beta}\beta + C_n^{p}p + C_n^{r}r + C_n^{\delta_V}\delta_V + C_n^{\delta_l}\delta_l$

3.5. Initial conditions of flight

Originally, the airplane performs a rectilinear steady flight with the given constant speed. For this condition, we can take:

$$p = q = r = 0 \qquad \beta = 0 \qquad \Phi = 0$$
$$\gamma = \Theta - \alpha = 0 \qquad \dot{V} = \dot{\alpha} = \dot{\beta} = \dot{p} = \dot{q} = \dot{r} = \dot{\Theta} = \dot{\Phi} = 0$$

In order to satisfy these conditions, the resultant foce and moment acting on the airplane must be equal to zero

$$\begin{aligned} P_{xa}\sin\alpha + (P_{za} - mg)\cos\alpha = 0 \\ T - P_{xa}\cos\alpha + (P_{za} - mg)\sin\alpha = 0 \end{aligned} \tag{3.7}$$

After necessary transformations, equations for the steady flight angle of attack α $(3.7)_1$ and indispensable thrust T $(3.7)_2$ are obtained. Knowing the airplane angle of attack α, we determine the elevator displacement angle δ_{H0}, so the coefficient of pitching moment is equal to zero.

4. Simulation of wing transverse vibrations

In simulation ot the wing vibration, the model of M28 "Bryza" Polish airplane with strut-braced wings was used. Along the span, the wing has varying cross-section areas (different moments of inertia), mass (different mass loads) as

well as varying aerodynamic loads. Some assumptions were made in order to simplify the model of wing vibrations such as:

- the wing has a constant cross-section area along its span;
- the wing is a fixed-free beam supported at y_L (y_P) from the wing root (airplane symmetry plane);
- the wing operates under a continuous aerodynamic load, invariant along the span;
- moments of inertia and moments of deviation are constant through the simulation.

On the basis of the above assumptions, the bending moment causes its parabolic-like deflection (Fig. 3.). Because of the scope of this paper, the problem of finding the frequency of structural vibrations and their amplitude has not been developed.

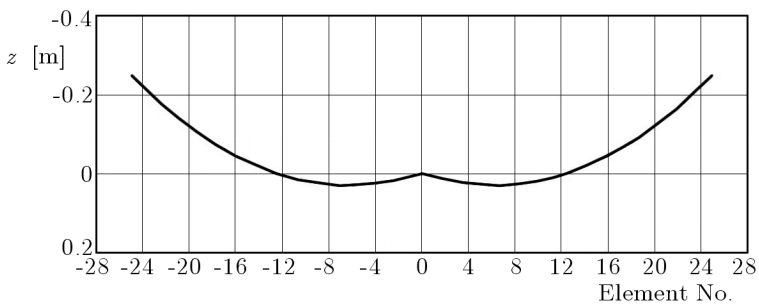

Fig. 3. Projection of the deflected wing (along the flight direction)

In the process of numerical simulation, the wing is divided into 50 evenly distributed elements. Because of the wing taper and sweep, each element has a different area and point of application of the aerodynamic force. The aerodynamic force is applied at the 25% chord of the considered wing element. The distance between the centre of the wing element and the airplane symmetry plane may be obtained according the formula below

$$y_{lok}(ne) = \pm\Big(\frac{\Delta l}{2} + (ne-1)\Delta l\Big) \tag{4.1}$$

where "+" refers to the right half of the wing, and the "−" to the left half; Δl is the width (span) of the wing element; ne – number of the wing element.

Considering a given element of the vibrating wing, one needs to determine the local angle of attack (further named: AOA). Assuming that the airfoil chord is parallel to the airplane longitudinal axis Ox, the total angle of attack

of the wing element (according to Fig. 4.) is equal to the sum of the airplane AOA and the change of AOA generated by the wing vertical movement during transverse vibrations. The above may be written as

$$\alpha_i(t) = \alpha_0(t) \pm \Delta\alpha_i(t) \qquad \pm \Delta\alpha_i(t) = \arcsin\Big(\frac{\pm V_{zi}(t)}{V(t)}\Big) \tag{4.2}$$

where: "+" indicates that the element moves "downward", and "−" "upward"; α_0 is the airplane angle of attack; $\Delta\alpha_i$ – change of AOA produced by transverse vibrations; α_i – current AOA value of the element.

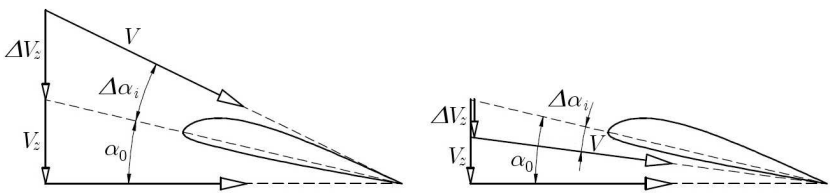

Fig. 4. Vertical velocity and AOA of the wing element

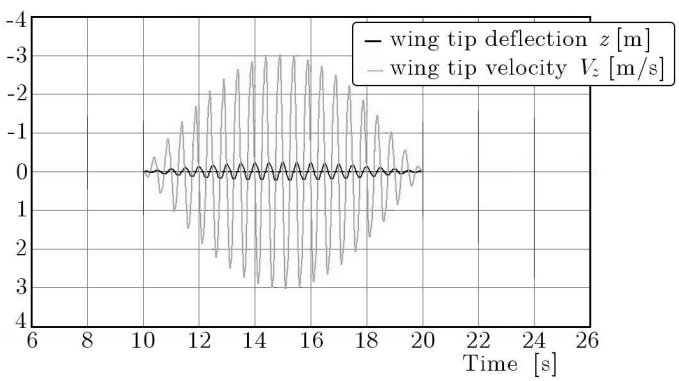

Fig. 5. Wing tip displacement and vertical velocity during transverse vibrations

The component calculated in equation $(4.2)_2$ produces the damping force for the vertical movement, which leads to a decrease in amplitude of vibrations.

The lift force for each wing element is derived. Calculations of the lift force take into consideration the wing sweep, local AOA value and distribution of circulation over the full span of the lifting surface. Figure 6 shows decomposition of the lift force along the wing span for aircraft velocity of 70 m/s.

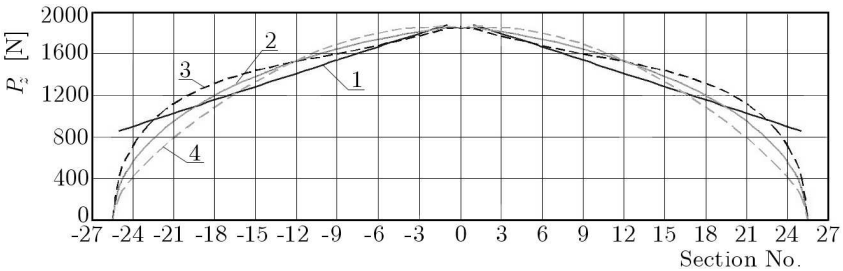

Fig. 6. Distribution of the wing lift force: 1 – elementary lift forces not including circulation; 2 – elementary lift forces including circulation; 3 – elementary lift forces for wing moving "downwards"; 4 – elementary lift forces for wing moving "upwards"

The total lift force produced by the wing of the aircraft is equal to

$$P_{za}^{total} = \int_{-l/2}^{l/2} P_{za} = \int_{-l/2}^{0} P_{za} + \int_{0}^{l/2} P_{za} = P_{za}^{L} + P_{za}^{P}$$

For determination of the lift force used in the considered model, the mentioned force may be obtained from equation (4.3)

$$P_{za}^{total} = P_{za}^{L} + P_{za}^{P} = \sum_{i=1}^{25} (P_{za}^{L})_i + \sum_{i=1}^{25} (P_{za}^{P})_i \tag{4.3}$$

The wing oscillates with a given frequency and amplitude. In each iteration of the numerical simulation, the vertical component z_{el} of the wing element position (Fig. 3.) and vertical velocity V_z are evaluated. Figure 5 presents trajectory of the wing tip and its normal velocity. For each element, the coefficients of drag, lift and pitching moment are determined.

5. Numerical analysis of perturbed airplane motion

In order to analyse the influence of wing transverse vibrations, using a computer code for solving the equations of motion, many cases of vibrations of the lift surfaces may be simulated. Because of the complex structure of the wing causing difficulties in estimating the vibration frequencies and amplitudes and the lack of airplane in-flight experimental data, the mentioned above values were evaluated (Issac, 1995).

Both cases of airplane motion with wing vibrations are based on the mathematical model described in Section 4. The steering vector $\boldsymbol{X}_{ST} = [\delta_H, \delta_V, \delta_l]^\top$ remains invariant in the analysis, which corresponds to a non-controlled flight condition.

The airplane performs a steady flight in smooth configuration (flaps on $\delta_{KL} = 0°$) with velocity of $V = 70\,\mathrm{m/s}$ ($\sim 252\,\mathrm{km/h}$) at altitude of $H = 1000\,\mathrm{m}$.

The initial turboprop engines thrust in the analysed time interval remains constant and has been determined on the base of steady flight condition (Eq. $(3.7)_2$). The static pitching moment is compensated by deflection of the horizontal control surface, which depends on the flight speed and is equal $\delta_{H0} = -0.44°$. The system of twelve nonlinear ordinary differential equations (2.11) and (2.15)-(2.17) was used to carry out the analysis.

Figures 7-14 present the results of airplane motion simulation with wing transverse vibrations covering two cases: (a) – "in phase" wing vibrations – both wing halves are moving in the same direction (along the airplane normal axis Oz); (b) – "in counter-phase" wing vibrations – wing halves are moving in the opposite direction.

Calculations were carried out for 300 seconds. The wing vibration occured after 10th seconds of simulation and disappeared at the 20th second. There was no pilot response, so the behaviour of the airplane itself was investigated.

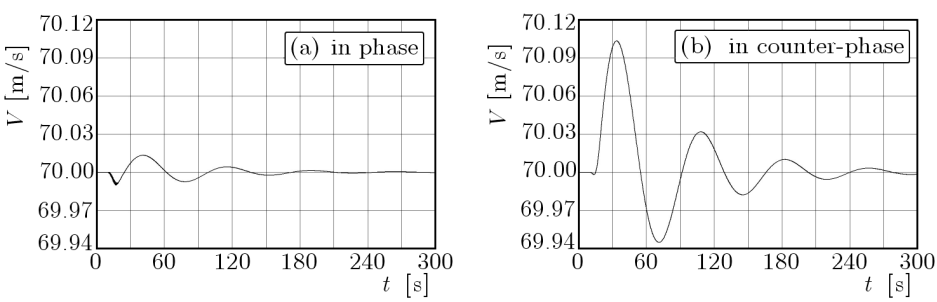

Fig. 7. Airplane velocity

Concerning the case (a), there is a slight loss in the airplane velocity (Fig. 7) and an increase in the angle of attack (Fig. 8) as the wing tips move upward at the very first moments of simulation. There is a temporary increase in the pitching moment resulting in the nose "pull up" (Fig. 10). Because both wing halves move in the same direction, the side forces produced by the lift force are equal and opposite. Thus a small side-slip angle is induced by the gyrostatic moment from engines rotors. Because of this, the roll and yaw angles

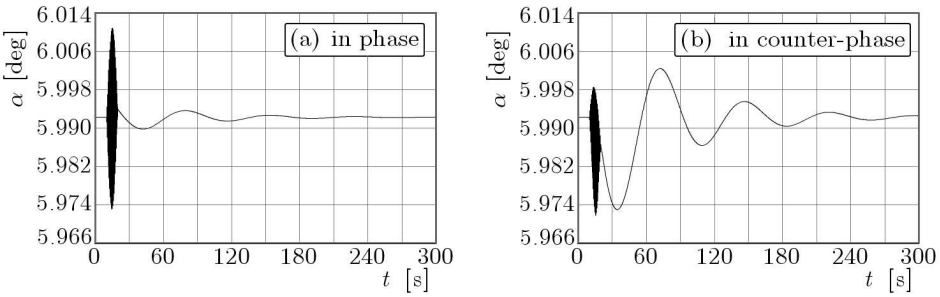

Fig. 8. Airplane angle of attack

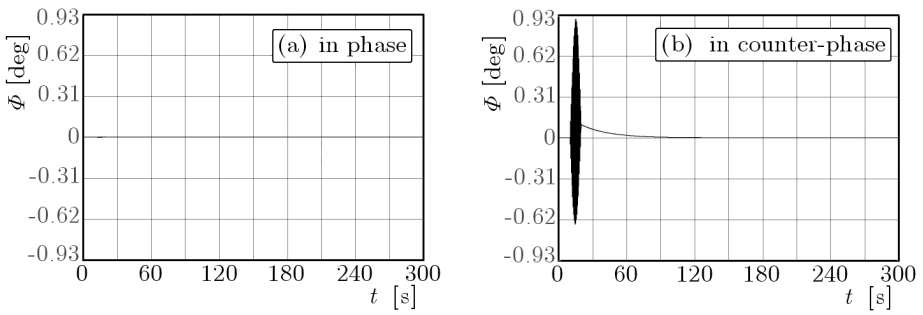

Fig. 9. Roll angle

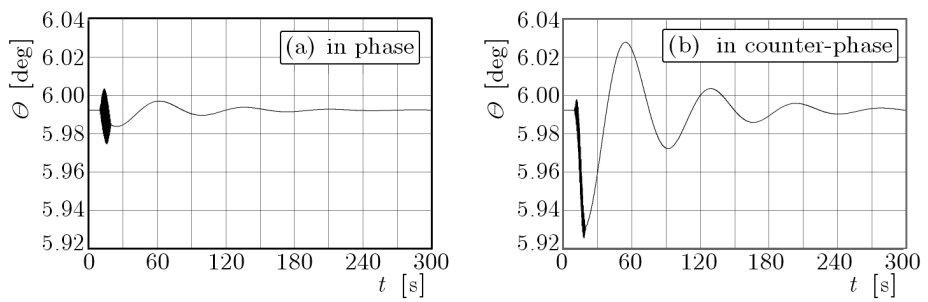

Fig. 10. Pitch angle

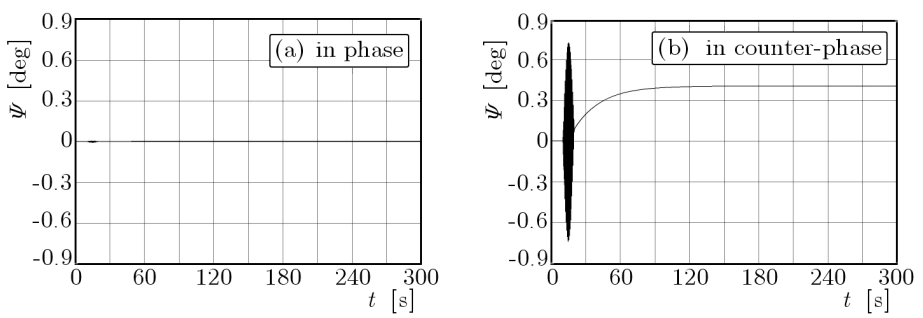

Fig. 11. Yaw angle

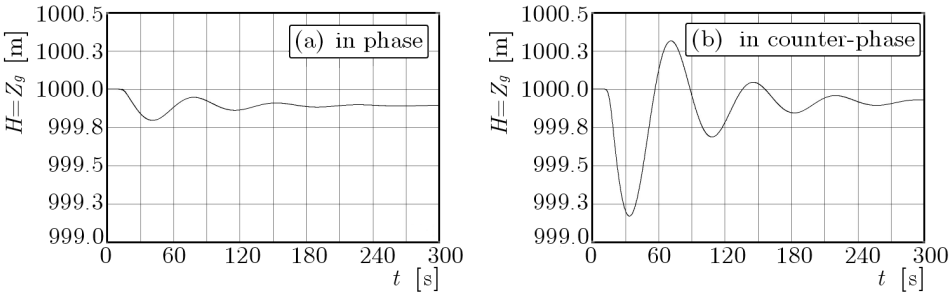

Fig. 12. Flight altitude

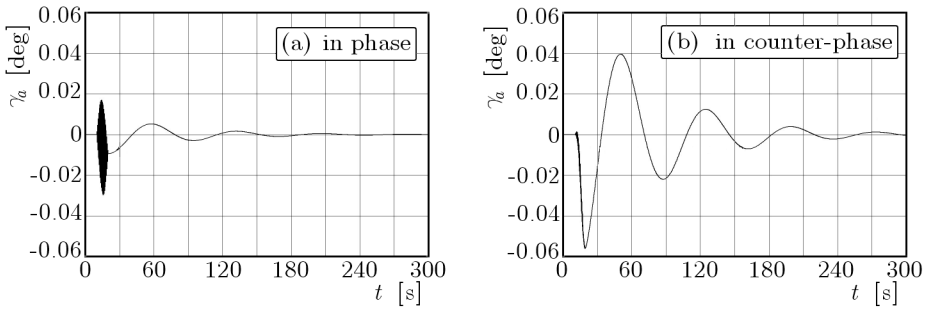

Fig. 13. Inclination angle

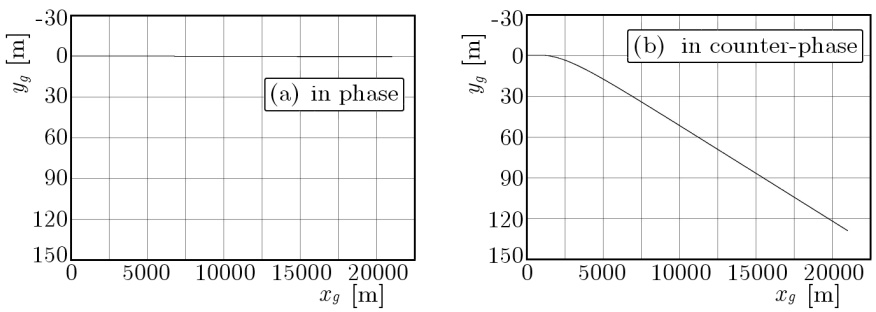

Fig. 14. Airplane trajectory

(Fig. 9 and Fig. 11) are small too (coupling of longitudinal and lateral motion). A decrease in the altitude (Fig. 12) and a small deviation from the initial direction of flight is observed (Fig. 14).

In case (b), when the wing halves move in the opposite direction, the above mentioned elementary side forces produce bigger side-slip angles as well as the roll and yaw. This leads to increasing deviation from the initial direction of flight. In comparison, there is a major velocity increase and a decrrease in the angle of attack at the very first moments of simulation than it was observed in case (a).

6. Conclusions

On the basis of results of numerical simulation, it is possible to state that a disturbed numerical model of M28 "Bryza" airplane remains stable because the parameters of motion return to their primary values:

- longitudinal stability → velocity, AOA and pitch angle return to the fixed values;
- lateral stability → roll angle returns to 0 and yaw angle is stabilized at a certain level.

Comparing two cases of wing transverse vibrations, it can be found that the "in counter-phase" wing vibrations have considerable influence on flight parameters. Because of the coupling of longitudinal and lateral motions, the growing side-slip angle produces bigger variations of the parameters. In both cases, a little drop of the altitude is noticed. During wing vibrations, all motion parameters oscillate, which results in unfavourable working conditions for many onboard systems, for instance the autopilot system. The vibrations badly influence the working environment for crew and travel comfort as well.

Wing vibrations have also significant effect on the airframe loading and durability. Varying loads lead to premature tear and wear of wing joints in the fuselage, suspensed devices and mountings of the control surfaces in the wing.

Deflections of the wing along the airplane normal axis Oz can produce additional forces acting on ailerons, which may result in bigger wing deflections and loads in the lateral control system.

References

1. Fiszdon W., 1962, *Mechanika lotu*, Cz. I, II, PWN, Warszawa
2. Hodges D.H., Pierce G.A., 2002, *Introduction to Structural Dynamics and Aeroelasticity*, Cambridge Aerospace Series, Cambridge
3. Issac J.C., 1995, *Sensitivity Analysis of Wing Aeroelastic Responses*, Virginia Polytechnic Institute, Blacksburg
4. Kowaleczko G., 2003, *Zagadnienie odwrotne w dynamice lotu statków powietrznych*, Wydawnictwo WAT, Warszawa
5. Krzyżanowski A., 1984, *Mechanika lotu*, skrypt WAT, Warszawa
6. Ostosławskij N.W., 1957, *Aerodinamika samoleta*, Oborongizdat, Moskwa

7. Szabelski K., Jancelewicz B., 2002, *Wstęp do konstrukcji śmigłowców*, WKŁ, Warszawa

8. Qin Z., 2001, *Vibration and Aeroelasticity of Advanced Aircraft Wings Modeled as Thin-Walled Beams*, Virginia Polytechnic Institute, Blacksburg

Wpływ drgań giętnych skrzydła na dynamiczne parametry lotu samolotu

Streszczenie

W pracy przedstawiono wyniki numerycznej symulacji drgań giętnych skrzydła samolotu dyspozycyjnego. Zastosowano klasyczny model matematyczny dynamiki ruchu samolotu, opisany przez układ dwunastu równań różniczkowych pierwszego rzędu. W celu uwzględnienia drgań skrzydła zamodelowano sposób przemieszczania się elementów skrzydła w samolotowym układzie współrzędnych oraz założono częstotliwość i amplitudę drgań skrzydła. Analizę przeprowadzono dla dwóch przypadków zginania skrzydła: zginanie połówek skrzydła w fazie i w przeciwfazie. Na podstawie analizy opracowano wnioski dotyczące własności dynamicznych samolotu podczas drgań jego powierzchni nośnych.

Manuscript received September 23, 2009; accepted for print October 14, 2009